

# The UV colours of high-redshift early-type galaxies: evidence for recent star formation and stellar mass assembly over the last 8 billion years

S. Kaviraj<sup>1\*</sup>, S. Khochfar<sup>1</sup>, K. Schawinski<sup>1</sup>, S. K. Yi<sup>2</sup>, E. Gawiser<sup>3</sup>, J. Silk<sup>1</sup>,  
S. N. Virani<sup>3</sup>, C. Cardamone<sup>3</sup>, P. G. van Dokkum<sup>3</sup> and C. M. Urry<sup>3</sup>

<sup>1</sup>*Department of Physics, University of Oxford, Keble Road, Oxford OX1 3RH, UK*

<sup>2</sup>*Yonsei University, Centre for Space Astrophysics, Seoul 120749, Korea*

<sup>3</sup>*Yale Center for Astronomy and Astrophysics, Yale University, New Haven, CT 06520-8121*

5 September 2007

## ABSTRACT

We combine deep optical and NIR ( $UBVRIzJK$ ) photometry from the Multiwavelength Survey by Yale-Chile (MUSYC) with redshifts from the COMBO-17 survey to perform a large-scale study of the rest-frame ultraviolet ( $UV$ ) properties of 674 high-redshift ( $0.5 < z < 1$ ) early-type galaxies, drawn from the Extended Chandra Deep Field South (E-CDFS). Galaxy morphologies are determined through visual inspection of Hubble Space Telescope (HST) images taken from the GEMS survey. We harness the sensitivity of the  $UV$  to young ( $< 1$  Gyrs old) stars to quantify the *recent* star formation history of early-type galaxies across a range of luminosities ( $-23.5 < M(V) < -18$ ). Comparisons to simple stellar populations forming at high redshift indicate that  $\sim 1.1$  percent of early-types in this sample are consistent with *purely* passive ageing since  $z = 2$  - this value drops to  $\sim 0.24$  percent and  $\sim 0.15$  percent for  $z = 3$  and  $z = 5$  respectively. Parametrising the recent star formation ('RSF') in terms of the mass fraction of stars less a Gyr old, we find that the early-type population as a whole shows a typical RSF between 5 and 13 percent in the redshift range  $0.5 < z < 1$ . Early-types on the broad  $UV$  'red sequence', show RSF values less than 5 percent, while the reddest early-types (which are also the most luminous) are virtually quiescent with RSF values of  $\sim 1$  percent. In contrast to their low-redshift ( $z < 0.1$ ) counterparts, the high-redshift early-types in this sample show a pronounced bimodality in the rest-frame  $UV$ -optical colour, with a minor but significant peak centred on the blue cloud. Furthermore, star formation in the most active early-types is a factor of 2 greater at  $z \sim 0.7$  than in the local Universe. Given that evolved sources of  $UV$  flux (e.g. horizontal-branch stars) should be absent at  $z > 0.5$ , implying that the  $UV$  is dominated by young stars, we find compelling evidence that early-types of all luminosities form stars over the lifetime of the Universe, although the bulk of their star formation is already complete at high redshift. This 'tail-end' of star formation is measurable and not negligible, with luminous ( $-23 < M(V) < -20.5$ ) early-types potentially forming 10-15 percent of their mass since  $z = 1$ , with less luminous early-types ( $M(V) > -20.5$ ) potentially forming 30-60 percent of their mass after  $z = 1$ . This, in turn, implies that intermediate-age stellar populations should be abundant in local early-type galaxies, as expected in hierarchical cosmology.

**Key words:** galaxies: elliptical and lenticular, cD – galaxies: evolution – galaxies: formation – galaxies: fundamental parameters

## 1 INTRODUCTION

The star formation histories (SFHs) of early-type galaxies have historically posed a significant challenge, with the exact mechanism of their formation the subject of

\* E-mail: skaviraj@astro.ox.ac.uk

intense and controversial debate in modern astrophysics. The classical ‘monolithic collapse’ hypothesis followed the model of Eggen et al. (1962) for the formation of the Galaxy. Refined and implemented by others (e.g. Larson 1974; Chiosi & Carraro 2002), this model postulated that stellar populations in early-type galaxies form in short, highly efficient starbursts at high redshift ( $z \gg 1$ ) and evolve purely passively thereafter. The optical properties of early-type populations and their strict obedience to simple scaling relations are indeed remarkably consistent with such a simple formation scenario. The small scatter in the early-type ‘Fundamental Plane’ (e.g. Jorgensen et al. 1996; Saglia et al. 1997) and its apparent lack of evolution with look-back time (e.g. Forbes et al. 1998; Peebles 2002; Franx 1993, 1995; van Dokkum & Franx 1996), the homogeneity (e.g. Bower et al. 1992) and lack of redshift evolution in their optical colours (e.g. Bender 1997; Ellis et al. 1997; Stanford et al. 1998; Gladders et al. 1998; van Dokkum et al. 2000) and evidence for short ( $< 1$  Gyr) star formation timescales in these systems, deduced from the over-abundance of  $\alpha$  elements (e.g. Thomas et al. 1999), all indicate that the bulk of the stellar population in early-type galaxies did indeed form at high redshift ( $z > 2$ ).

While it reproduces the optical properties of early-type galaxies remarkably well, a monolithic SFH does not sit comfortably within the currently accepted LCDM galaxy formation paradigm, in which galaxy mass is thought to accumulate over the lifetime of the Universe, through both quiescent and merger-driven star formation. Following the seminal work of Toomre (1977), who showed that most galaxy collisions end in mergers and postulated the formation of spheroidal systems as end-products of such merging activity, the mechanics of galaxy interactions (e.g. Barnes & Hernquist 1992a,b; Hernquist 1993) and their link to the formation of early-type systems (see e.g. Barnes & Hernquist 1996, or Bender (1996) for an observational perspective) has been studied in considerable detail. Current semi-analytical models of galaxy formation within the LCDM framework create early-type galaxies through major mergers, where the mass ratio of the merging progenitors is 3:1 or lower. The constituent stellar mass of early-type systems is predicted to form both in mergers and interactions and through quiescent star formation in their progenitors over the lifetime of the Universe (e.g. Cole et al. 2000; Hatton et al. 2003; Khochfar & Burkert 2003).

While theoretical arguments may be compelling, the strongest evidence for the role of interactions in shaping early-type galaxy evolution and inducing coincident star formation comes from observation. While individual examples of merger remnants can be clearly seen in the local Universe (e.g. NGC 5128 (Israel 1998) and IC 4200 (Serra et al. 2006)), fine structure, which is indicative of recent interactions is not uncommon in the nearby early-type population. 40 percent of local ellipticals contain dust lanes (Sadler & Gerhard 1985), while over 75 percent contain nuclear dust and by implication gas (e.g. Tomita et al. 2000; Tran et al. 2001). The gas is often kinematically decoupled from the stars, indicating, at least in part, an external origin, e.g. through the accretion of a gas rich satellite (e.g. Sarzi et al. 2006). Up to two-thirds of nearby early-types contain shells and ripples (e.g. Malin & Carter 1983; van Dokkum 2005) and a significant fraction exhibit kin-

ematically decoupled cores (e.g. de Zeeuw et al. 2002), both of which are evidence for interactions in the recent past (e.g. Barnes & Hernquist 1992b). Moreover, fine structure and disturbed morphologies often coincide with signatures of recent star formation (e.g. blue broad-band colours), implying that such events are frequently accompanied by detectable amounts of star formation (e.g. Schweizer et al. 1990; Schweizer & Seitzer 1992) even at low redshift. While the detection of spatially resolved fine structure is possible only for galaxies in our local neighbourhood, signatures of recent star formation persist in the nearby galaxy population out to modest redshifts (e.g. Trager et al. 2000a,b; Fukugita et al. 2004).

While many of the recent efforts have centred on the nearby Universe, deep ground and space-based imaging have increasingly provided access to galaxy populations over the last ten billion years of look-back time. A significant fraction ( $\sim 30$  percent) of luminous early-type systems at high redshifts ( $0.4 < z < 0.8$ ) exhibit blue cores, indicative of merger-driven starbursts triggered by the accretion of low-mass gas-rich companions (Menanteau et al. 2001). Not unexpectedly, such blue cores are typically accompanied by emission and absorption lines characteristic of recent star formation (Ellis et al. 2001). A fundamental consequence of early-type evolution in the standard model is the gradual loss of late-type progenitors over a Hubble time (e.g. van Dokkum & Franx 2001; Kaviraj et al. 2005). Since late-types merge to form early-types, the early-type fraction is expected to decrease with increasing redshift, while the late-type fraction should show a corresponding increase. Numerous observational studies have detected this predicted evolution in the morphological mix of the Universe. While  $\sim 80$  percent of galaxies in the cores of local clusters have early-type morphology (Dressler 1980), a higher fraction of spiral (blue) galaxies have been reported in clusters at high redshift (e.g. Butcher & Oemler 1984; Dressler et al. 1997; Couch et al. 1998; van Dokkum et al. 2000; Margoniner et al. 2001; Andreon et al. 2004; Borch et al. 2006; Bundy et al. 2006), along with increased rates of merger and interaction events (e.g. Couch et al. 1998; van Dokkum et al. 1999). The fraction of blue galaxies evolves from a few percent in nearby ( $z < 0.1$ ) clusters to  $\sim 30$  percent at intermediate redshifts ( $z \sim 0.5$ ) and reaches  $\sim 70$  percent at high redshift  $z \sim 1$ , although the exact trend has some dependence on the cluster richness and magnitude limit adopted by the study in question. This is supported by recent results from large-scale surveys which suggest that the mass density on the red sequence (which is dominated by early-type systems) has doubled since  $z = 1$  (e.g. Bell et al. 2004; Faber et al. 2005). A significant body of observational evidence thus indicates that the SFHs of at least some early-type galaxies, and perhaps the early-type population as a whole, deviate strongly from the expectations of the monolithic collapse paradigm, both in terms of their structural evolution and the star formation experienced by them over a Hubble time.

The vast majority of work on early-type galaxies in the past has focussed on *optical* spectro-photometric data. A significant drawback of optical photometry is its lack of sensitivity to moderate amounts of recent star formation. While red optical colours do imply a high-redshift formation epoch for the bulk of the stars in early-type galaxies, the optical

spectrum remains largely unaffected by the minority of stellar mass that forms at low and intermediate redshift. As a result it is virtually impossible to resolve early-type SFHs over the last 8 billion years ( $0 < z < 1$ ), where the predictions of the two competing models diverge the most.

A first step towards resolving the SFHs over this timescale is to quantify the *recent star formation* (RSF) in early-type systems at  $z \sim 0$ . RSF can be efficiently traced using the rest-frame ultraviolet (*UV*) spectrum, which is sensitive to young, massive main sequence stars with ages less than  $\sim 1$  Gyr. The *UV* remains largely unaffected by the ‘age-metallicity degeneracy’ which plagues optical studies (Worthey 1994), allowing it to maintain its age sensitivity across a large range in metallicity and making it an ideal photometric indicator of RSF (Kaviraj et al. 2006c). Using a large sample of early-type galaxies detected by the GALEX *UV* space telescope, Kaviraj et al. (2006b) have recently shown that, contrary to the expectations of classical models (e.g Bower et al. 1992), nearby early-type galaxies show widespread RSF - at least 30 percent show blue *UV*-optical colours which cannot be achieved through the *UV* flux from old horizontal-branch (HB) stars (Yi et al. 1997, 1999) alone and require some RSF to be present in these systems. In fact, up to 90 percent of early-types in this sample have photometry that is consistent with RSF within the observational errors. Most importantly, Kaviraj et al. (2006b) have demonstrated that the early-type SFHs predicted by semi-analytical models in the  $\Lambda$ CDM framework provide excellent quantitative agreement with the observed *UV* photometry from GALEX and that monolithic models (where RSF can be driven solely by recycled gas from stellar mass loss) cannot reproduce the observed *UV* colours under reasonable assumptions for the chemical enrichment or star formation histories.

This study extends these results to high redshift by exploiting deep optical photometry to trace the rest-frame *UV* properties of early-type galaxies in the redshift range  $0.5 < z < 1$ . We harness the sensitivity of the *UV* to young stars to quantify the recent star formation history of early-types at high redshift. We combine our results with similar studies in the local Universe (Kaviraj et al. 2006b) to estimate the star formation history of the early-type population between  $z = 0$  and  $z = 1$  (i.e. the last 8 billion years of look-back time) and test their conformity to scenarios for their formation, especially the classical ‘monolithic collapse’ hypothesis.

We note that the *UV* properties of the E-CDFS galaxy population have previously been explored by Wolf et al. (2005, W05 hereafter), who looked at the contributions to the *UV* luminosity density from various morphological classes of galaxies in the redshift range  $0.65 < z < 0.75$ . The study presented here differs from W05 in several ways. While W05 studied the *UV* flux around  $2800\text{\AA}$ , our emphasis is on the *UV* spectrum around  $2300\text{\AA}$  which is more sensitive to recent star formation. Furthermore, we deal exclusively with the early-type population over a larger redshift range  $0.5 < z < 1$  and explicitly quantify the recent star formation in each galaxy in our sample. Nevertheless, W05 forms an important benchmark for the results presented here and we draw parallels between the two studies throughout the course of this work.

## 2 EARLY-TYPE GALAXIES IN THE EXTENDED CHANDRA DEEP FIELD SOUTH

### 2.1 The data

Numerous ongoing optical surveys are now deep and wide enough to provide access to the rest-frame *UV* flux of entire galaxy populations at redshifts beyond  $\sim 0.5$ . The Extended Chandra Deep Field South (E-CDFS), in particular, contains a plethora of deep surveys which provide panchromatic data over a large range in redshift, spanning the X-rays through to the infrared wavelengths. Three recent optical surveys in E-CDFS, MUSYC (Gawiser et al. 2006)<sup>1</sup>, COMBO-17 (Wolf et al. 2004)<sup>2</sup> and GEMS (Rix et al. 2004)<sup>3</sup>, provide the full suite of deep optical photometry, redshifts and morphologies required to accurately study the early-type population in the rest-frame *UV* at high redshift.

The MUSYC survey provides deep *UBVRIz'JK* imaging of E-CDFS, to AB depths of  $U, B, V, R = 26.5$  and  $J, K = 22.5$ . The MUSYC broad-band (*UBRI*) data combines COMBO-17 imaging with those from the ESO Deep Public Survey (Arnouts et al. 2001). COMBO-17 provides 17 filter photometry, including 12 medium-band filters, and accurate photometric redshifts due to its large filter set. The redshift accuracies are  $\sim 1$  percent for  $R < 21$ ,  $\sim 2$  percent for  $R \sim 22$  and better than 10 percent for  $R < 24$ . GEMS provides *V* and *z*-band HST-ACS images of galaxies in E-CDFS out to  $z \sim 1$ , from which morphologies can be robustly deduced, due to the superb angular resolution of the ACS camera. The GEMS survey traces at least the rest-frame *B*-band within our target redshift range ( $0.5 < z < 1$ ), so that morphological K-corrections are minimal within this redshift range.

In this study, we combine deep broad-band photometry from MUSYC and photometric redshifts from COMBO-17 with morphologies from GEMS to study the early-type population in E-CDFS in the rest-frame *UV* within the redshift range  $0.5 < z < 1$ . The lower limit of our target redshift range ( $z \sim 0.5$ ) is determined by the epoch at which the optical *U*-band ( $\sim 3600\text{\AA}$ ) traces the rest-frame near-*UV* ( $\sim 2300\text{\AA}$ ). The upper limit ( $z \sim 1$ ) is driven primarily by the fiducial depth of GEMS, but also by the epoch to which redshifts can be reliably determined from COMBO-17 and the need to avoid large morphological K-corrections. In addition, we adopt a magnitude limit of  $R = 24$ , because COMBO-17 redshifts are robust down to this limit and the GEMS images are bright enough to perform reasonably accurate morphological classification.

We note that, although MUSYC and COMBO-17 offer similar broad-band filter sets, MUSYC is significantly deeper than COMBO-17 in its broad-band imaging - e.g. the MUSYC *U*-band is 2 magnitudes deeper than its COMBO-17 counterpart. It is the depth of this imaging, particularly in the *U* and *B*-band filters, that makes it possible to trace the rest-frame near-*UV* accurately. Since errors in the optical photometry propagate through the analysis into the estimated rest-frame photometry, a robust determination of the

<sup>1</sup> <http://www.astro.yale.edu/MUSYC/>

<sup>2</sup> [http://www.mpia.de/COMBO/combo\\_index.html](http://www.mpia.de/COMBO/combo_index.html)

<sup>3</sup> <http://www.mpia.de/GEMS/home.htm>

rest-frame colours and their associated parameters requires deep optical imaging. We also note that, wherever possible, we substitute COMBO-17 photometric redshifts with spectroscopic redshifts from the VVDS survey (Le Fèvre et al. 2004). In addition, for galaxies that fall within the GOODS (Giavalisco et al. 2004) field in E-CDFS, we use GOODS imaging instead of GEMS since the GOODS pointings are deeper.

Finally, we note that (Type 1) AGN are removed using the COMBO-17 ‘QSO’ flag and by removing objects that are detected in the E-CDFS X-ray point-source catalog of Virani et al. (2006). The fraction of early-types in this X-ray catalog is small - only 15 out of the 674 objects that are morphologically classified as early-type (see the next section) have detections in Virani et al. (2006).

## 2.2 Morphological classifications

The advent of large-scale space and ground-based surveys in a wide variety of wavelengths is giving us unprecedented access to statistically large populations of galaxies across a variety of redshifts and environments. However, the size of the galaxy samples poses a challenge when morphological classification is necessary. Early-type galaxies can be selected using automated pipelines that isolate objects on the basis of their two-dimensional light distributions. For example, Bernardi et al. (2000) have constructed a catalog of  $\sim 9000$  low-redshift early-type galaxies, selected using a combination of SDSS pipeline parameters. This catalog contains galaxies with a high  $i$ -band concentration index ( $r_{50}/r_{90} > 2.5$ ) and in which a deVaucouleurs fit to the surface brightness profile is significantly more likely than an exponential fit. Visual inspection of this catalog indicates that, while such automated prescriptions are efficient at selecting a reasonably robust early-type galaxy sample, they do admit a significant fraction of contaminants (e.g. face-on disks, edge-on spirals and late-type galaxies with weak spiral features).

In this study we simply opt for visual inspection of the individual HST images of MUSYC galaxies in E-CDFS. Although it is arguably subjective and logistically difficult to implement on large samples of galaxies, visual inspection minimises the contamination in the early-type galaxy sample studied in this paper. For the sample studied in this paper, the superb angular resolution ( $\sim 0.05''$ ) of the HST facilitates morphological classification, since small-scale structure is better resolved than ground-based images which typically have resolutions of  $\sim 1''$ . At the imaging depth of the GEMS and GOODS surveys (from which the HST imaging of the MUSYC galaxies is derived) and within the magnitude limit adopted in this study, morphological classification of early-type galaxies should be ‘safer’ than that performed using standard SDSS images in Kaviraj et al. (2006b), who studied the  $UV$  properties of a sample of low-redshift ( $z < 0.1$ ) early-type galaxies drawn, through visual inspection, from the SDSS.

In this study, we split our parent galaxy sample (comprised of 4498 objects) into three main morphological classes. The first are ‘relaxed early-type’ galaxies which show an unperturbed spheroidal morphology with no detectable signs of spiral features. We refer to this class simply as ‘early-type’ hereafter. The second are ‘possible early-types’

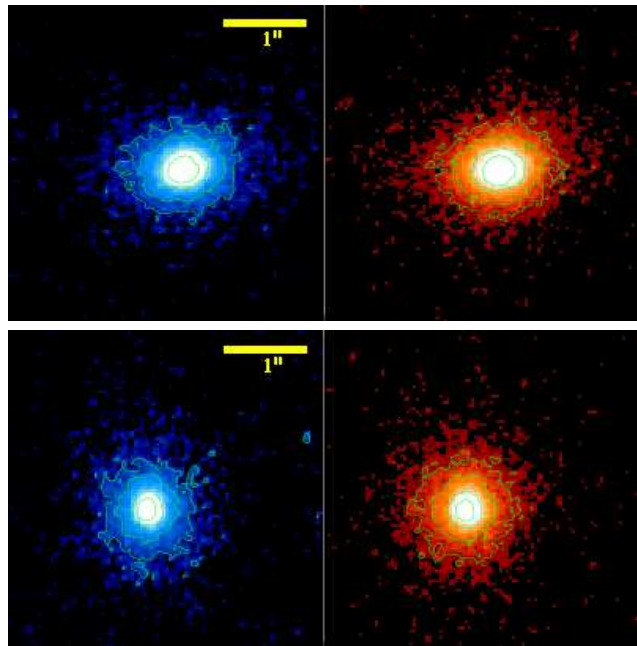


**Figure 1.** Example GEMS images of galaxies classified as ‘early-type’ in this study. The left-hand column shows the  $V$ -band image (rest-frame  $U$ -band), while the right-hand column shows the  $z$ -band image (rest-frame  $V$ -band). The top panel shows an early-type at  $z = 0.596$ , while the bottom panel shows an early-type at  $z = 0.720$ . The redshifts are photometric and taken from the COMBO-17 survey.  $1''$  corresponds to  $\sim 7$  kpc at  $z \sim 0.7$ .

which appear early-type but whose spheroidal morphology is uncertain. As our analysis indicates below, it is likely that these galaxies are indeed contaminants, as the distribution of their properties does not follow that of the (relaxed) early-type population. Separating these objects is clearly important and makes our ‘early-type’ classification safer. The third class, which we label ‘late-type’, includes all objects which do not fall into the above categories. We also identify a fourth category of ‘disturbed galaxies’ (e.g. tidal tails and double cores) which are potential *progenitors* of early-type galaxies and which are the subject of a forthcoming paper.

Figures 1 and 2 show example images of the ‘early-type’ and ‘possible early-type’ categories. We show GEMS images of each galaxy in both the  $V$ -band (rest-frame  $U$ -band; left-hand column) and the  $z$ -band (rest-frame  $V$ -band; right-hand column). The morphological classification was carefully performed by SK, using both bands and checked against composite images released by the GEMS collaboration. The process was repeated five times and the fraction of galaxies in the ‘possible early-type’ category became stable between the third and fourth passes. This process yields 674 early-type galaxies and 100 ‘possible early-types’, out of a parent sample of 4498 objects.

To check the quality of the visual inspection we compare our classification results (for galaxies in the redshift range  $0.65 < z < 0.75$ ) to those of W05, who also performed visual inspection of their E-CDFS galaxy sample with a similar magnitude cut of  $m(R) < 24$ . Unfortunately W05 do not provide a breakdown of the number of objects in each of their morphological classes so the comparison is performed by counting up the relevant number of objects in the up-

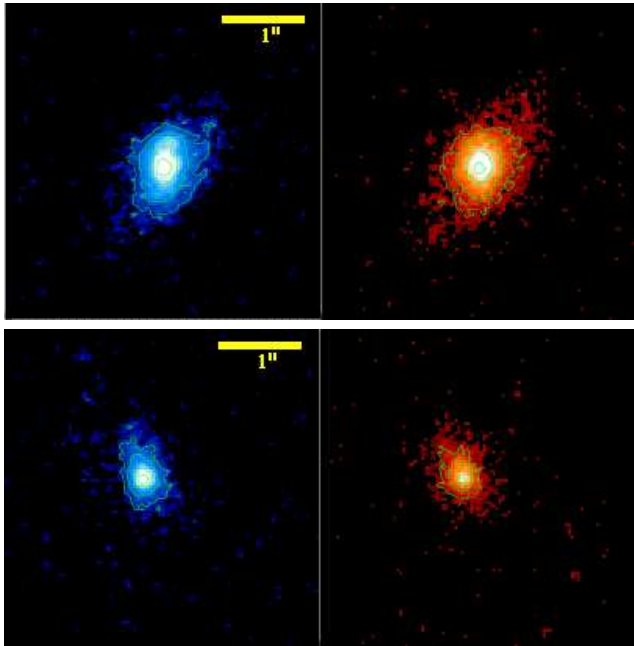


**Figure 2.** Example GEMS images of galaxies classified as ‘possible early-type’ in this study. The left-hand column shows the V-band image (rest-frame U-band), while the right-hand column shows the z-band image (rest-frame V-band). The top panel shows a possible early-type at  $z = 0.637$ , while the bottom panel shows a possible early-type at  $z = 0.607$ . The redshifts are photometric and taken from the COMBO-17 survey.  $1''$  corresponds to  $\sim 7$  kpc at  $z \sim 0.7$ .

per left panel of Figure 5 and dividing by the total number of objects in the W05 sample. Since early-types on the red sequence can be easily identified (the red sequence is dominated by early-types in all studies) we simply compare the fraction of early-types in the blue cloud selected by the two studies. We find that blue ( $M_{280} - M_V < 1$ ) early-types in W05 comprise  $\sim 9.3$  percent of their parent galaxy population. In comparison blue early-types in our study, selected using the criterion  $(NUV - r) < 4$ , comprise 6.8 percent of the population. This figure rises to 8.4 percent if we also consider blue galaxies (again using  $(NUV - r) < 4$ ) in the possible early-type category. Since the colour cut employed to separate the red sequence from the blue cloud is somewhat arbitrary, we do not find the small difference in the blue early-type fractions particularly compelling and are satisfied that the visual inspection in these two studies correspond well. In fact, it is likely that the classification performed in this study is slightly more conservative than that used by W05.

### 2.3 Estimation of rest-frame photometry and derived parameters

We estimate the rest-frame photometry and star formation histories (SFHs) of individual galaxies by comparing the multi-wavelength photometry of each observed MUSYC object with synthetic galaxy populations, generated in the framework of the standard model. Synthetic populations are generated using the semi-analytical model of Khochfar & Burkert (2003). Cosmological parameters used

for the background cosmology are taken from the three-year WMAP observations (Spergel et al. 2007):  $\Omega_m = 0.241$ ,  $\Omega_\Lambda = 0.759$ ,  $h = 0.732$ ,  $\sigma_8 = 0.761$ . Merger trees are calculated using the extended Press-Schechter formalism with a mass resolution of  $5 \times 10^9 M_\odot$ . The model reproduces merger statistics and galaxy properties accurate down to  $1 \times 10^{10} M_\odot$  (Khochfar & Burkert 2001). Baryonic physics is implemented as described in Khochfar & Burkert (2005) and Khochfar & Silk (2006) and star formation histories include the self-consistently calculated contributions of all progenitor galaxies. AGN feedback is implemented according to the phenomenological approach described in Schawinski et al. (2006), in which gas cooling is halted in galaxies hosting black holes more massive than a critical black hole mass.

A library of synthetic photometry is constructed by combining each of  $\sim 15,000$  model galaxies with a single metallicity in the range  $0.1Z_\odot$  to  $2.5Z_\odot$  and a measure of the dust content parametrised by a value of  $E(B - V)$  in the range 0 to 0.5. Photometric predictions are generated by combining each model combination with the stellar models of Yi (2003) and the MUSYC filter transmission curves convolved with the correct atmospheric conditions. Each library thus contains  $\sim 750,000$  model galaxies and their associated predicted photometry in the MUSYC filter set.

Since our observed dataset spans a large redshift range ( $0.5 < z < 0.1$ ), synthetic libraries are generated at redshift intervals of  $\delta z = 0.02$ . Each MUSYC object is studied using the library which is closest to it in redshift. A fine redshift grid minimises ‘K-correction-like’ errors in the estimated rest-frame colours that are induced by the redshift offset between the observed object and the library used to analyse it. Each observed galaxy is compared to every model in the library and the likelihood ( $\exp -\chi^2/2$ ) of each model extracted using the value of  $\chi^2$ , computed in the standard way. We estimate rest-frame colours (e.g.  $U - V$ ,  $NUV - r$ ) by taking the average colour of all models which yield ‘good fits’ ( $\chi_R^2 < 2$ ). We take the standard deviation of these model colours as a measure of the error in the rest-frame photometry. Finally, we construct an ‘average SFH’ for each observed galaxy, by combining the SFHs of all models in the library weighted by their individual likelihoods. The recent star formation (RSF), which is the focus of this study and which we define as the *mass fraction of stars formed within the last Gyr in the rest-frame of the galaxy*, is calculated from this average SFH. Note that the  $NUV$  passband employed in this study corresponds to the GALEX  $NUV$  filter which covers the spectral range  $1750\text{\AA} - 2750\text{\AA}$  and has an effective wavelength of  $2271\text{\AA}$ .

## 3 DERIVED REST-FRAME UV-OPTICAL COLOURS OF THE E-CDFS GALAXY POPULATION

### 3.1 Sources of UV flux in early-type galaxies

Analysis of the rest-frame UV properties of early-type galaxies in the local Universe ( $0 < z < 0.2$ ) is complicated by the fact that their UV spectrum may contain contributions from both young and old stellar populations. Core helium burning stars on the horizontal branch (HB), thought to be the

primary cause of the ‘UV upturn’ phenomenon in massive elliptical galaxies (Yi et al. 1997, 1999), emit efficiently in the  $UV$  spectral ranges. Thus the potential ‘contamination’ of the  $UV$  spectrum from old HB stars must be taken into account before estimating the contribution from young stellar populations, complicating the robust detection of recent star formation in early-type systems.

The onset of the HB typically takes 9-10 Gyrs (e.g. Yi et al. 1999), depending on the metallicity of the population. Thus, a key benefit of the analysis presented here is that, given the lower redshift limit ( $z = 0.5$ ) employed in this study, HB stars should not have time to develop and contribute to the  $UV$  spectrum<sup>4</sup>. The lack of evolved  $UV$ -emitting stellar populations therefore makes our conclusions more robust than can be achieved by corresponding studies in the local Universe (e.g. Kaviraj et al. 2006b).

### 3.2 Rest-frame colour-magnitude relations

We begin by presenting the estimated rest-frame photometry for the galaxy population in E-CDFS within the redshift range  $0.5 < z < 1$ . Figure 3 shows the rest-frame  $(U - V)$  (top) and  $(NUV - r)$  (bottom) CMRs of the galaxy population in the E-CDFS in the redshift range  $0.5 < z < 1$ . Red circles indicate early-type galaxies and green circles represent possible early-types. The small black dots indicate late-type systems. The  $(U - V)$  colours are in excellent agreement with the COMBO-17 results of Bell et al. (2004) for the E-CDFS. Note that magnitudes given here are in the AB system while COMBO-17 reports magnitudes in the VEGAMAG system. The conversion between the two filter systems is  $(U - V)_{MUSYC} \sim (U - V)_{COMBO17} + 0.75$ . The  $NUV$  passband is taken from the GALEX filterset and the  $r$ -band filter is taken from the SDSS. These filters are chosen to facilitate comparison with the results of Kaviraj et al. (2006b) at low redshift. Figure 4 presents the distribution of one-sigma errors for the derived rest-frame  $(U - V)$  and  $(NUV - r)$  colours shown in Figure 3. Median uncertainties are indicated using the solid red lines. The median uncertainties in  $(U - V)$  is  $\sim 0.08$ , while the median uncertainty in  $(NUV - r)$  is  $\sim 0.2$ <sup>5</sup>. In Figure 5 we split the rest-frame  $(U - V)$  and  $(NUV - r)$  CMRs into three redshifts bins to show their evolution with look-back time.

Similar to the early-type population at low redshift (see Figure 4 in Kaviraj et al. 2006b), the high-redshift early-types in this study show a broad red sequence, which spans almost three magnitudes in the  $(NUV - r)$  colour. The origin of this broadness is the high sensitivity of the  $UV$  to young stars - the  $UV$  photometry is able to resolve small differences in the recent SFH resulting in the broad distribution of colours on the red sequence. Conversely, the insensitivity of optical colours to such low levels of RSF results in the significantly tighter optical red sequence that is apparent in the top panel of Figure 3. We note that a similar result was found by W05, who found a red sequence spanning 1.5

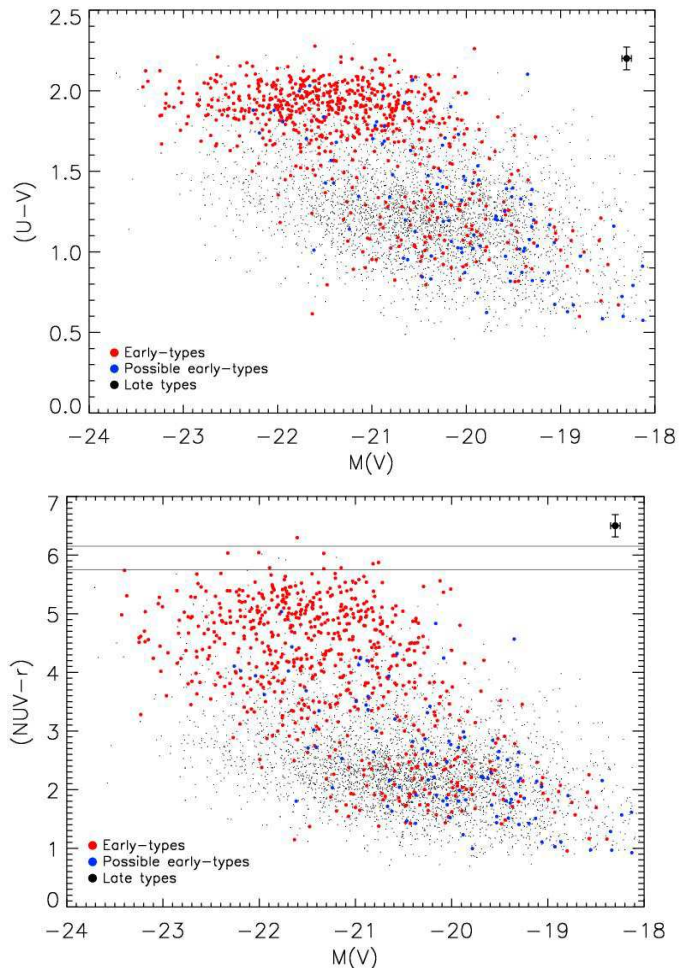


**Figure 3.** TOP PANEL: The rest-frame  $(U - V)$  CMR of the galaxy population in the E-CDFS in the redshift range  $0.5 < z < 1$ . BOTTOM PANEL: The rest-frame  $(NUV - r)$  CMR of the galaxy population in the E-CDFS. The  $NUV$  passband is taken from the GALEX filterset and the  $r$ -band filter is taken from the SDSS. The filters are chosen to facilitate comparison with the results of Kaviraj et al. (2006b) at low redshift. The solid horizontal lines indicate the expected position of a dustless simple stellar population which forms at  $z = 3$  with solar metallicity and is observed at  $z = 0.5$  (upper line) and  $z = 1$  (lower line).

mag in the rest-frame  $(2800 - V)$  colour (see their Figure 5). The fact that the  $(2800 - V)$  red sequence is narrower is expected, since it is not as sensitive to recent star formation as its  $(NUV - r)$  counterpart.

### 3.3 Comparisons to the monolithic collapse hypothesis

It is instructive to first compare the expectations of the classical monolithic scenario, in which galaxies evolve *completely passively* since high redshift, to the rest-frame CMRs of the E-CDFS population. For example, the Yi (2003) models predict that a (dustless) simple stellar population (SSP) of solar

<sup>4</sup> Assuming formation redshifts of 3 and 5, the maximum age of stellar populations are  $\sim 6.3$  and  $\sim 7.3$  Gyrs respectively

<sup>5</sup> For comparison, the observational errors in the GALEX (Martin et al. 2005)  $UV$  photometry of low-redshift galaxies is  $\sim 0.25$  magnitudes.

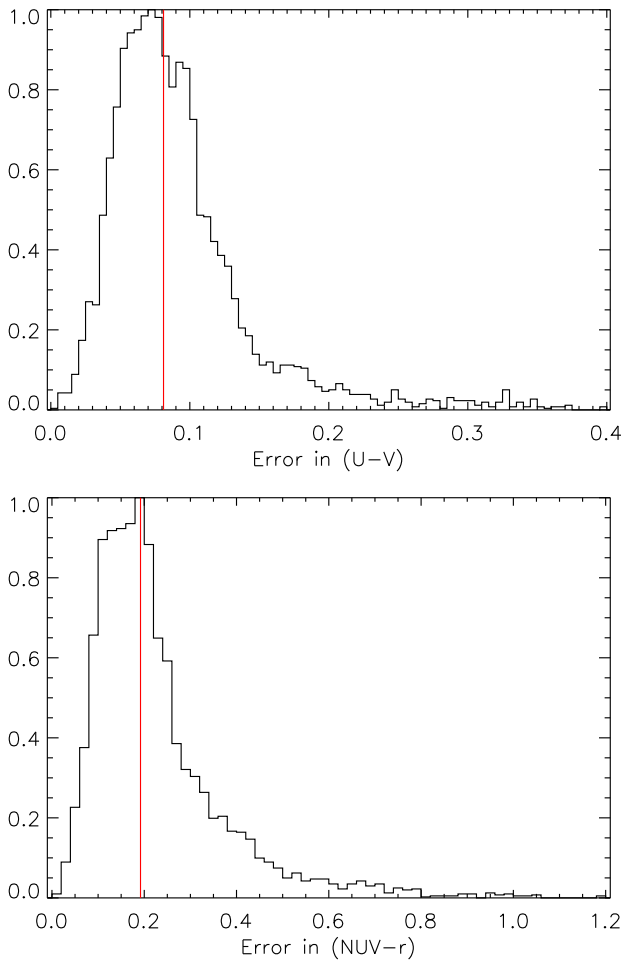


**Figure 4.** Errors in the derived rest-frame  $U - V$  (top) and  $NUV - r$  (bottom) colours of the galaxy population in E-CDFS (shown in Figure 3). Median uncertainties are indicated using the solid red lines. The median uncertainty in  $(U - V)$  is  $\sim 0.08$  while the median uncertainty in  $(NUV - r)$  is  $\sim 0.2$ .

metallicity which forms at  $z \sim 3^6$ , will have  $(NUV - r) \sim 6.15$  and  $(NUV - r) \sim 5.75$  at  $z \sim 0.5$  and  $z \sim 1$  respectively. As an independent check we calculate the position of this dustless  $z = 3$  SSP using the Bruzual & Charlot (2003) stellar models and find that its corresponding position remains virtually unchanged at  $(NUV - r) \sim 6.12$  and  $(NUV - r) \sim 5.71$  for  $z \sim 0.5$  and  $z \sim 1$  respectively.

Inspection of Figure 3 indicates that early-types in general are incompatible with such a simple SFH, since virtually all early-types in this sample (even those in the red sequence) lie blueward of  $(NUV - r) \sim 5.75$ . We make this comparison more robust by comparing the  $(NUV - r)$  colour of each galaxy in our sample to SSPs forming at high redshift ( $z = 2, 3, 5$ ). We apply the median metallicity of the galaxy in question to the SSP but note that our re-

<sup>6</sup> The choice of  $z = 3$  is motivated by optical studies (e.g. Bower et al. 1992, 1998) which have ‘age-dated’ cluster early-type populations using optical photometry. The SSP age estimates from such studies consistently indicate a formation redshift greater than  $z = 2$ .

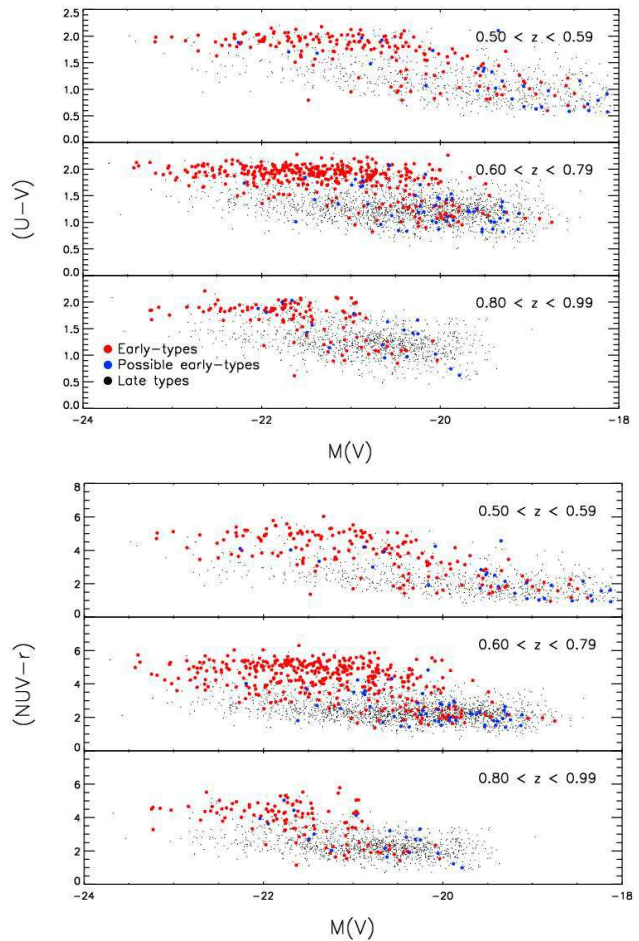


**Figure 5.** TOP PANEL: The rest-frame  $(U - V)$  CMR as a function of redshift. BOTTOM PANEL: The rest-frame  $(NUV - r)$  CMR as a function of redshift.

sults remain virtually unchanged if we simply assume solar metallicity throughout. A galaxy that has an  $(NUV - r)$  colour redder, within errors, than that of an SSP forming at  $z = z_f$  is clearly consistent with being passively evolving since  $z = z_f$ . Thus, by comparing the  $(NUV - r)$  colour of each galaxy to SSPs at  $z_f = 2, 3$  and  $5$  we can estimate the fraction of early-types which could be considered to be ageing passively (i.e. evolving ‘monolithically’) since these formation redshifts. We find that within the sample studied here,  $\sim 1.1$  percent of early-types are consistent with purely passive ageing since  $z = 2$ . This value drops to  $\sim 0.24$  percent and  $\sim 0.15$  percent for  $z = 3$  and  $z = 5$  respectively. This result includes the individual errors in  $(NUV - r)$  for each galaxy and is therefore robust. We therefore find that, based on this SSP comparison, virtually none of the early-type galaxies in this sample exhibit photometric properties consistent with purely passive ageing since  $z = 2$ .

While the SSP criterion used above to estimate the fraction of potentially passively evolving galaxies is justifiable and driven by previous observational studies, it is reasonable to ask whether the choice of a single metallicity affects our interpretation, as real galaxies - even those that might evolve monolithically - must contain a metallicity distribution (MF) in their stellar populations. We note first that MFs derived from semi-analytic models of early-type

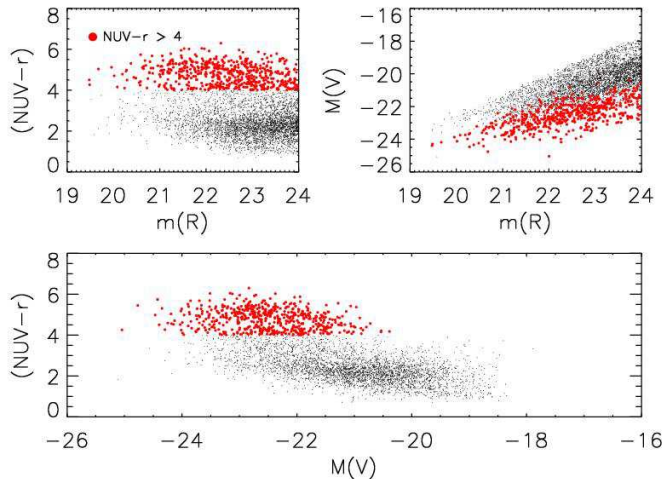


**Figure 6.** Although red ( $NUV-r > 4$ ) galaxies are well-sampled in apparent  $R$ -band magnitude (top left), the  $K$ -corrections for red objects are larger (top right), resulting in these systems shifting further to the *left* in the rest-frame CMR (bottom panel). This induces a lack of red galaxies in the rest-frame CMR as shown in bottom panel. To populate the faint red end in the rest-frame CMR requires galaxies which have  $m(R) < 24$ . Hence the lack of red galaxies is caused indirectly by our magnitude limit ( $m(R) = 24$ ). Recall, however, that our magnitude limit is chosen to ensure reliability of the redshift estimates and morphological classifications.

galaxy formation, which are potentially more realistic, are very sharply peaked at solar or super-solar values, depending on the mass of the early-type in question (Nagashima & Okamoto 2006; Seong-Hee Kim, priv. comm.), implying that the single metallicity assumption is a reasonable one.

In a more relevant study, Kaviraj et al. (2006c, see their Section 6) explored hypothetical ( $NUV-r$ ) colours of ‘monolithically evolving’ scenarios using chemical enrichment models. Monolithic galaxies were constructed by requiring high star-formation efficiencies at high redshift, resulting in red optical colours and high values of alpha-enhancement as observed in the local early-type population (e.g. Thomas et al. 1999). Note that, by construction, these models contain metallicity distributions. Comparison of the ( $NUV-r$ ) colours at  $z \sim 0.5$  and  $z \sim 1$  of such monolithic scenarios indicates that they are consistent with the SSP colours we have used in our analysis. Depending on the strength of the galactic wind allowed in these models the ( $NUV-r$ ) colours can, in fact, be redder (by as much as  $\sim 0.2$  mag) than a solar metallicity SSP, especially in deep potential wells where metals are more efficiently retained. Therefore, the fractions of potentially quiescent galaxies derived above, using comparisons to SSPs, should be reasonably robust.

### 3.4 The lack of faint red galaxies

The rest-frame CMRs in Figure 3 show a distinct lack of *red* galaxies at the low luminosity end. We explain this briefly using Figure 6 which indicates that, while red ( $NUV-r > 4$ ) galaxies are well-sampled in apparent  $r$ -band magnitude (top left), the  $K$ -corrections for red objects are larger (top right), resulting in these systems shifting further to the *left*

in the rest-frame CMR. This induces a lack of red galaxies at the low luminosity end of the rest-frame CMR, as shown in bottom panel. To populate this low luminosity end therefore requires galaxies which have  $m(R) > 24$ . Hence, the lack of red galaxies is indirectly caused by our magnitude limit of  $m(R) = 24$ . Recall, however, that this magnitude limit is chosen to ensure the reliability of the redshift estimates and robustness of the morphological classifications and thus such low luminosity red galaxies are beyond the scope of this study.

## 4 QUANTIFYING THE RECENT STAR FORMATION IN THE E-CDFS GALAXY POPULATION

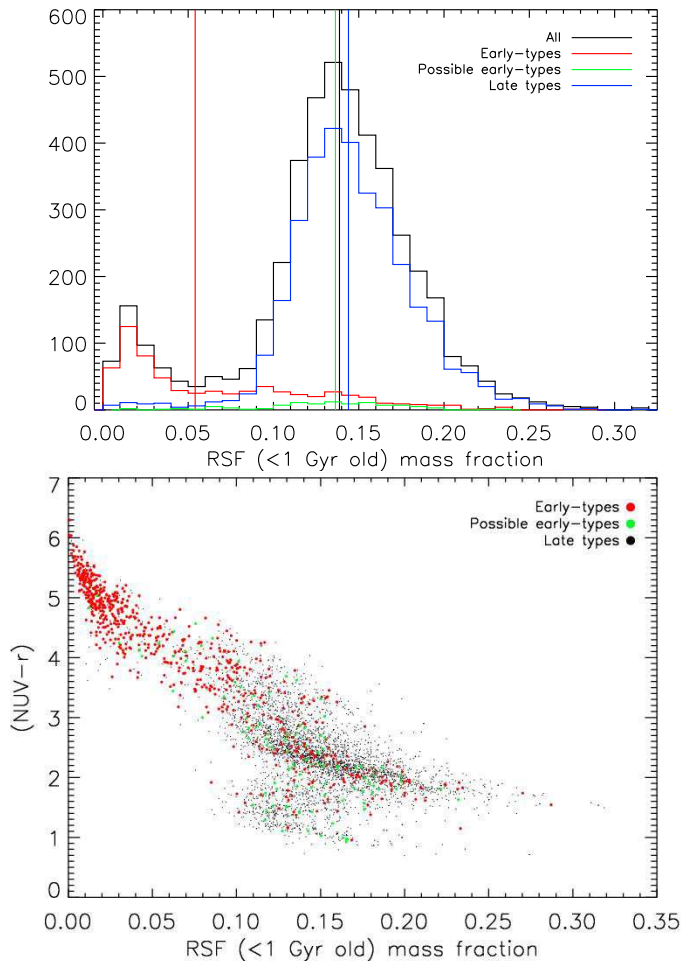
The main focus of this study is to quantify the recent star formation (RSF) in the high redshift ( $0.5 < z < 1$ ) early-type population. Recall that we define the RSF as the mass fraction of stars that form in a galaxy, within the last 1 Gyr of look-back time in its rest frame. The choice of timescale is driven by the fact that the rest-frame  $UV$  is most sensitive to stars less than  $\sim 1$  Gyr old.

Figure 7 (top panel) shows the histogram of RSF values for all galaxies in the E-CDFS population. The RSF distribution is bimodal. The population as a whole shows a median RSF of  $\sim 14$  percent (marked using the solid black line in Figure 7) while the maximum value is  $\sim 30$  percent. Late types (blue) span a wide range of RSF values from  $\sim 5$  percent up to  $\sim 30$  percent of the galaxy mass. Median values of RSF (indicated by the vertical lines in the inset) are  $\sim 5.5$  percent for early-types (red),  $\sim 13.8$  percent for the ‘possible’ early-type population (green) and  $\sim 14.4$  percent for late-type galaxies (black). The late-type population typically shows three times the RSF of their early-type counterparts. We also note that the bulk of the early-type population, which preferentially populate the red sequence ( $NUV-r > 4$ ), have RSF values lower than the median value of 5.5 percent (the modal value is  $\sim 2$  percent) - the slightly high median is caused by the long tail to high RSF values.

The bottom panel of Figure 7 shows the rest-frame ( $NUV-r$ ) colour plotted against the RSF and split by galaxy morphology. The small peak at low RSF values, apparent in the RSF distribution (top panel), is completely dominated by early-type galaxies (red points in the bottom panel). A robust separation exists between morphologies in this parameter space, with early-types overwhelmingly dominating the clump of galaxies with very low ( $< 5$  percent) RSF values.

It should be noted that the value of the RSF mass fraction does not give any indication of the *profile* of the recent SFH. Galaxies with similar RSF mass fractions can have widely disparate ( $NUV-r$ ) colours, depending on the exact shape of their recent SFHs. For example, a galaxy experiencing a burst of star formation nearly 1 Gyr in the past will be redder in the ( $NUV-r$ ) colour than a galaxy experiencing a burst of similar intensity which takes place within the last 100 Myrs. Hence, while a correlation clearly must exist between RSF and the ( $NUV-r$ ) colour, the variation in the recent SFHs induces a ‘broadening’ in the ( $NUV-r$ ) vs. RSF relation, which is apparent in Figure 7.





**Figure 7.** TOP PANEL: Histogram of recent star formation (RSF) for galaxies in the E-CDFS population. Recall that RSF is defined as the mass fraction of stars formed within the last Gyr of look-back time in the rest-frame of the galaxy. Solid vertical lines indicate the median values of the distributions for different morphologies. The RSF is bimodal with the small peak at very low RSF values completely dominated by (luminous) early-type galaxies (see below). BOTTOM PANEL: The rest-frame  $(NUV - r)$  colour plotted against the RSF. A good separation exists between morphologies in this parameter space, with early-types (red) dominating the clump of galaxies with very low RSF values. Late type galaxies span a wide range in RSF values from  $\sim 5$  percent up to  $\sim 30$  percent of the total galaxy mass. The broadening of the relation at high RSF values is caused by widely disparate recent SFHs within the galaxy population (see the text in Section 4 for further discussion).

A spread in dust and metallicity values may also contribute to this broadening, but their contribution is minor compared to that caused by the variation in recent SFHs within the galaxy population. In particular, we find some galaxies in the  $(NUV - r)$  vs. RSF parameter space, with RSF values between 10 and 20 percent, which are displaced from the main locus of galaxies. These objects show bluer  $(NUV - r)$  colours for the same values of RSF as galaxies on the main locus because they have encountered a very recent period of star formation, probably as a result of an interaction event, within the last 0.5 to 1 Gyr. We also observe that, not un-

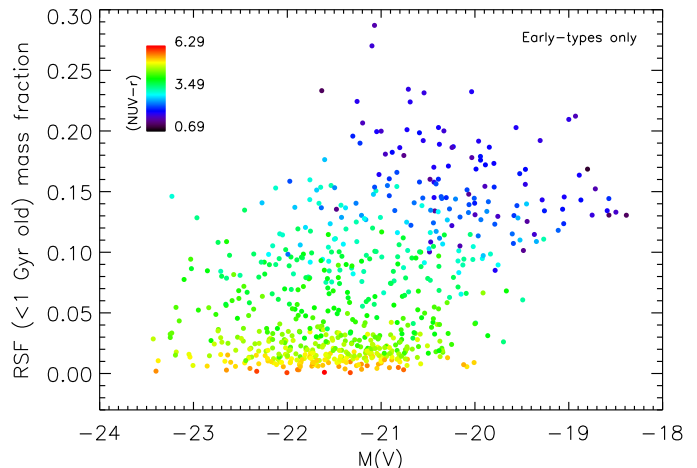


**Figure 8.** RSF as a function of the absolute  $V$ -band luminosity of the early-type galaxies, with galaxies colour-coded according to their rest-frame  $(NUV - r)$  colour. Note that the other morphological classes are omitted from this figure for clarity.

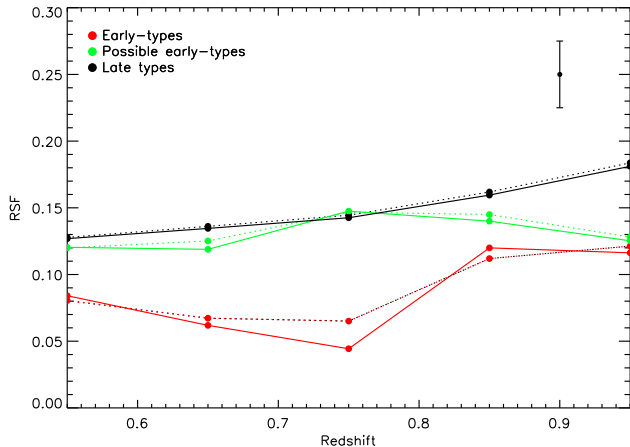
expectedly, the correlation between  $(NUV - r)$  colour and RSF becomes tighter for low values of RSF, since very small starbursts, even at small look-back times, are not able to significantly perturb the  $(NUV - r)$  colour from that due to a largely old population.

In Figure 8 we show the RSF as a function of the absolute  $V$ -band luminosity of the early-type galaxies, with galaxies colour-coded according to their  $(NUV - r)$  colour. Note that the other morphological classes are omitted from this figure for clarity. A well-populated locus with low RSF values (less than 5 percent) exists across a wide range in luminosities ( $-23.5 < M(V) < -20$ ). The high RSF tail, apparent in the top panel of Figure 7, is not restricted only to faint early-type galaxies. A minority ( $\sim 10$  percent) of luminous early-types ( $-23.5 < M(V) < -21$ ) exhibit high values of RSF, greater than 10 percent. Galaxies fainter than  $M(V) = -20$  typically have very high RSF values (between 10 and 25 percent). Finally, there is a broad trend of increasing RSF towards fainter galaxies, a manifestation of the ‘downsizing’ phenomenon recently studied in the literature (Cowie et al. 1996; Bundy et al. 2006).

In Figure 9 we show the evolution of RSF with redshift (across all the morphological classes). Solid lines in this figure represent median values of RSF (in keeping with results presented earlier) while the dotted lines represent mean values. Within the errors, there is a slight indication that the RSF increases with redshift, from  $\sim 7$  percent at  $z = 0.5$  to  $\sim 13$  percent at  $z = 1$ . The typical uncertainty in the RSF values is  $\sim 2.5$  percent.

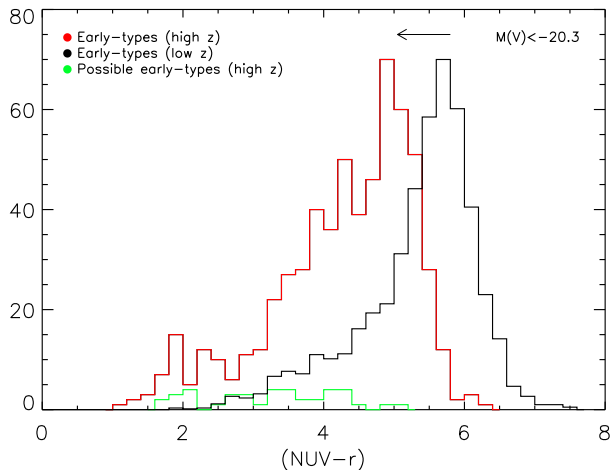
#### 4.1 Comparison to the local Universe

Figure 10 compares the high-redshift  $(NUV - r)$  colours in this study (solid red line) to their counterparts at low redshift (solid black line) from Kaviraj et al. (2006b). In contrast to the low-redshift early-type population studied by Kaviraj et al. (2006b), high-redshift early-types show a pronounced bi-modality around  $(NUV - r) \sim 3$ , with the blue peak centred on the blue cloud shown in Figure 3. The



**Figure 9.** Evolution of RSF with redshift for all the morphological classes. Solid lines in this figure represent median values of RSF (in keeping with results presented earlier) while the dotted lines represent mean values.

Note that most of the redshifts in this study are photometric (see text for details).



**Figure 10.** Comparison of the high-redshift ( $NUV - r$ ) colours in this study (solid red line) to their counterparts at low redshift (solid black line) from Kaviraj et al. (2006b). The histograms are normalised to the same peak value to facilitate comparison. Also shown are the histograms for possible early-types (green) and disturbed galaxies which could be progenitors of early-types at lower redshift (blue). The arrow indicates the change in the ( $NUV - r$ ) colour of a solar metallicity SSP population which forms at  $z = 3$  from a redshift of  $z \sim 0.7$  to  $z \sim 0.1$ , which approximately represent the median redshifts in both studies.

peak of the high-redshift ( $NUV - r$ ) distribution shows a relative shift from its low-redshift counterpart (shown using the arrow in Figure 10) which corresponds to the passive ageing of a simple stellar population forming at  $z = 3$ . This indicates that the bulk of stellar population in early-type galaxies (on the red sequence) is overwhelmingly old.

The blue peak contains  $\sim 15$  percent of the early-type population, with an average RSF of  $\sim 11$  percent. In comparison, the bluest 15 percent of the low-redshift early-type population, studied by Kaviraj et al. (2006b), has an average

RSF of  $\sim 6$  percent. The intensity of (recent) star formation in the most active early-types has therefore halved between  $z \sim 0.7$  (which is median redshift of this study) and present-day.

#### 4.2 The dust-age degeneracy in $UV$ colours - robustness of the RSF estimation

As mentioned before, the  $UV$  spectrum is largely unaffected by the age-metallicity degeneracy (Kaviraj et al. 2006c) and therefore the age estimation remains robust within the metallicity range considered in this study ( $0.1Z_{\odot}$  to  $2.5Z_{\odot}$ ). However, the  $UV$  is far more sensitive to the presence of dust than the optical spectrum. The GALEX  $NUV$  filter for example, on which the rest-frame analysis in this paper is based, is three times more sensitive to dust than the optical  $V$ -band filter, assuming standard dust extinction laws (e.g. Cardelli et al. 1989; Calzetti et al. 2000). It is thus possible to ‘redden’ the  $UV$  colour by adding arbitrary amounts of dust to the system. Therefore, as an independent check of the robustness of the parameter estimation we demonstrate that the derived SFH parameters for red early-type galaxies do not involve significant amounts of dust, since these galaxies should be red due to a lack of young stars rather than due to heavy internal extinction.

In Figure 11 (top panel) we show the distribution of ( $NUV - r$ ) colours for late-types, early-types and also the red early-type population. We define ‘red’ early-types using an arbitrary colour cut at ( $NUV - r$ ) = 5. Recall that the red envelope position for a (dustless) purely old SSP lies at ( $NUV - r$ )  $\sim 6.15$  and ( $NUV - r$ )  $\sim 5.75$  at  $z \sim 0.5$  and  $z \sim 1$  respectively. The ( $NUV - r$ ) = 5 criterion therefore picks objects that are less than 1 magnitude away from the red envelope position in ( $NUV - r$ ). This selection threshold, although somewhat arbitrary, is reasonable, given the broadness of the  $UV$  red sequence.

The bottom panel of Figure 11 shows the RSF distributions for these three categories of objects. The median value of RSF in the red early-type population is  $\sim 1.3$  percent. This demonstrates explicitly that the parameter estimation does not favour dusty SFHs for red early-type systems, notwithstanding the large range of  $E(B - V)$  values available to it. The spectra of red early-type galaxies are consistent with them being quiescent systems.

## 5 SUMMARY AND DISCUSSION

We have combined deep optical and NIR  $UBVRIz'JK$  photometry, photometric redshifts and HST imaging from the MUSYC, COMBO-17 and GEMS surveys respectively to perform a large-scale study of the rest-frame  $UV$  properties of the early-type galaxy population in E-CDFS, in the redshift range  $0.5 < z < 1$ . Our study is one of the first of its kind to study the rest-frame  $UV$  flux around  $2300\text{\AA}$  at high redshift and provides both a useful comparison to similar studies performed at low redshift and a benchmark for future work that might exploit the rest-frame  $UV$  spectral ranges to study distant early-type galaxies.

By comparing the observed photometry with synthetic populations, generated in the framework of the standard model, we have computed the rest-frame  $UV$  and optical

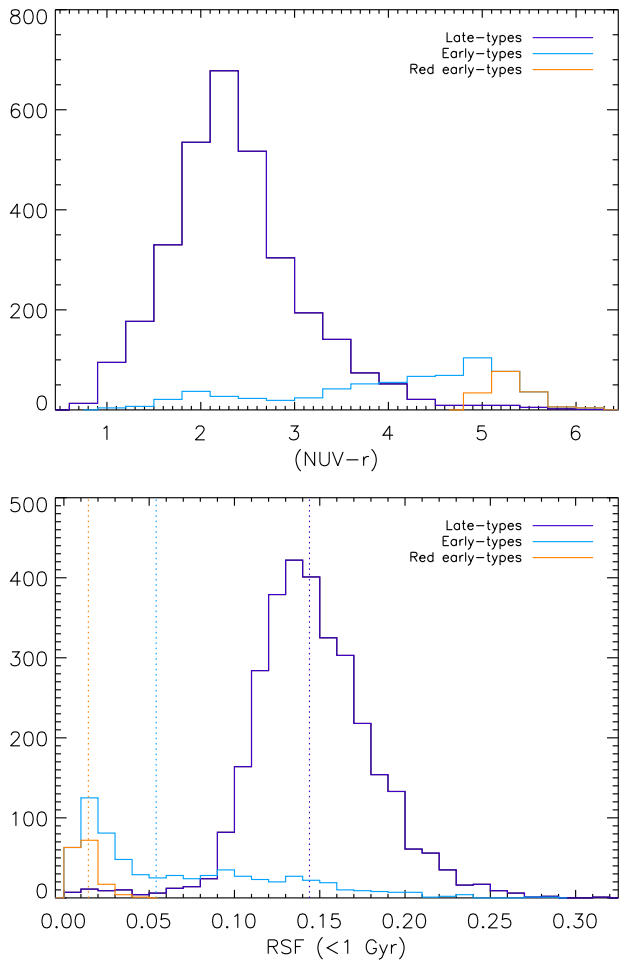


**Figure 11.** TOP PANEL: Distribution of  $(NUV - r)$  colours for late-types, early-types and red early-type population, defined using an arbitrary colour cut at  $(NUV - r) = 5$ . BOTTOM PANEL: RSF distributions for the three categories of objects described above. Median values are shown using the dotted vertical lines.

colours of the E-CDFS galaxy population and quantified, for each E-CDFS galaxy, the stellar mass contributed by recent star formation (RSF), defined as the mass fraction in stars less than 1 Gyr old in the rest-frame of the galaxy. The sensitivity of the rest-frame  $UV$  to young stars allows us to detect RSF at levels as low as 1 percent of the total mass of the galaxy and robustly constrain the star formation history (SFH) of galaxies within the last Gyr.

We find that, similarly to the low-redshift ( $0 < z < 0.1$ ) early-type population, high-redshift early-types display a broad ‘red sequence’ which spans almost three magnitudes in the  $(NUV - r)$  colour. The origin of this broadness is the high sensitivity of the rest-frame  $UV$  to young stars. Small differences in the proportion of young stars in largely quiescent galaxies broadens the  $UV$  red sequence (bottom panel in Figure 3), while the optical red sequence remains relatively narrow (top panel in Figure 3) because optical colours remain virtually unaffected by small mass fractions of young stars. By comparing the  $(NUV - r)$  colour-magnitude relation of the E-CDFS galaxy population (top panel in Figure 3) to the expected  $(NUV - r)$  colours of simple stellar populations forming at high redshift ( $z = 2, 3, 5$ ), we have

deduced that  $\sim 1.1$  percent of early-types in this sample are consistent (within errors) with *purely* passive ageing since  $z = 2$ . This value drops to  $\sim 0.24$  percent and  $\sim 0.15$  percent for  $z = 3$  and  $z = 5$  respectively.

The early-type population *as a whole* exhibits a typical RSF between 5 and 13 percent in the redshift range  $0.5 < z < 1$ , while the early-types on the broad red sequence ( $NUV - r > 4$ ) typically show RSF values less than 5 percent. The reddest early-types (which are also the most luminous) are virtually quiescent with RSF values of  $\sim 1$  percent. Within the errors, there is a slight indication that the RSF increases with redshift, from  $\sim 7$  percent at  $z = 0.5$  to  $\sim 13$  percent at  $z = 1$ . Note that the typical uncertainty in the RSF is  $\sim 2.5$  percent.

Comparison of our results to a corresponding study of early-type galaxies in the local Universe (Kaviraj et al. 2006b) indicates that, in contrast to their low-redshift counterparts, the early-type population in E-CDFS shows a pronounced bimodality in the  $(NUV - r)$  colour distribution around  $(NUV - r) \sim 3$  (Figure 10). The peak of the high-redshift  $(NUV - r)$  distribution shows a relative shift from its low-redshift counterpart which is close to what might be expected from the passive ageing of a simple stellar population forming at high redshift (indicated by the arrow in Figure 10). This indicates that the *bulk* of the stellar population in early-type galaxies, at least on the red sequence, is overwhelmingly old. The blue peak in the high-redshift  $(NUV - r)$  distribution contains  $\sim 15$  percent of the early-type population, with an average RSF of  $\sim 11$  percent. In comparison, the bluest 15 percent of the low-redshift early-type population has an average RSF of  $\sim 6$  percent, indicating that star formation activity in the most active early-types has halved between  $z = 0.7$  and present day.

We note that evolved stellar populations capable of emitting in the  $UV$ , e.g. horizontal branch stars, should not be present in galaxies in this study, since there is insufficient time for them to appear, given the lower redshift cut employed here ( $z = 0.5$ ). Hence, the  $UV$  flux seen in the galaxy population studied here comes *exclusively* from young stars, making our results more robust than can be achieved by similar studies at low redshift, where contamination of the  $UV$  spectrum from old populations has to be taken into account before the contribution from young populations can be estimated.

This study has demonstrated that the early-type population, in general, is not composed of galaxies that have been evolving completely passively since high redshift. Taken together with the widespread RSF found in low-redshift early-types, we find compelling evidence that early-type galaxies of all luminosities form stars over the lifetime of the Universe, although the bulk of their star formation is already complete at high redshift. Contrary to conclusions from some past studies, which were focussed mainly on the optical wavelengths that are insensitive to recent star formation, this ‘tail-end’ of star formation in early-type galaxies is measurable and not negligible. Since the timescale of this study is  $\sim 2.5$  Gyrs, a simple extrapolation (from RSF values in Figure 8) indicates that luminous ( $-23 < M(V) < -20.5$ ) early-type galaxies may typically form up to 10-15 percent of their mass after  $z = 1$  (with a tail to higher values), while their less luminous ( $M(V) > -20.5$ ) counterparts form 30-60 percent of their mass in the redshift range. These values

are probably overestimated since the intensity of star formation is seen to decrease between  $z = 0$  and redshifts probed by this study. This tail-end of star formation should exist in *intermediate-age* (3-8 Gyr old) stellar populations in early-type galaxies at present day.

It is worth noting here that the early-type galaxy sample studied here is drawn from a variety of environments. The largely photometric nature of the redshifts employed in this study makes it difficult to separate galaxies in dense regions from their field counterparts. However, galaxies in dense regions are predicted to complete their mass assembly and star formation significantly faster than counterparts in the field (Kaviraj et al. 2006a). Hence, we should be careful about applying the conclusions derived above to galaxy populations in general. For example, although 10 to 15 percent of the stellar mass in luminous early-types may typically form after  $z = 1$ , the corresponding values for cluster galaxies will be at least a factor of 2 lower, given their faster evolution.

We note that our results and, in particular, the implied mass buildup in the early-type population in the redshift range  $0 < z < 1$  inferred from our analysis, are in good agreement with the results of van der Wel et al. (2007), who studied star formation in high-redshift ( $0.85 < z < 1.15$ ) early-type galaxies in the CDF-S using GOODS-MIPS infrared imaging. The majority of their sample is in the (optical) red sequence (see their Figure 4) and their results indicate that (a) the early-type population is dominated by evolved stellar populations (b) most early-types are not affected by dust-obscured star formation or AGN and (c) the increase in the early-type stellar mass density in the redshift range  $0 < z < 1$  is  $14 \pm 7$  percent. (a), (b) and (c) are clearly consistent with our results for early-types on the *UV* red sequence and (d) compares well with our estimate of 10-15 percent for the mass buildup expected for luminous early-types which inhabit the red sequence.

While the analysis presented in this study has quantified the RSF in the E-CDFS early-type population, we have not explored the possible sources of young stars in these galaxies. Although a comprehensive study of these sources is beyond the scope of this paper (and will be dealt with in future work), we use the results of our analysis to speculate on the RSF channels that might be at work in the early-type population.

Several plausible sources of low-level star formation exist, which could, either individually or collectively, explain the broadness of the *UV* red sequence. An obvious source of star formation is internally recycled gas from stellar mass loss. For standard IMFs, a substantial (20-30 percent) fraction of the stellar mass may be returned to the ISM. However, only stars formed from recycled gas entering the ISM within the last Gyr will contribute to the *UV*. Kaviraj et al. (2006c; see their Section 6) have suggested that RSF from internal mass loss is an order of magnitude too small ( $\sim 0.2$  percent; see their Figure 28, bottom left panel) than what is observed (a few percent) in red early-types in this study. It is therefore likely that internal mass loss plays a negligible role in broadening the red sequence and that other sources of gas are required to produce the observed RSF in these systems.

Condensation from the extensive hot gas reservoirs hosted by massive early-type galaxies may provide an ad-

ditional source of cold gas in these systems. While feedback sources (e.g. AGN and supernovae) might be expected to maintain the temperature of the hot gas reservoir and evaporate infalling cold material in the most massive haloes (Binney 2004), this process may not be fully efficient, allowing some gas condensation to take place, which could then result in low-level star formation as the cold gas settles in the potential well.

Merger and accretion events provide an alternative source of young stars. The small levels of RSF in red sequence early-types indicate that the star formation in these galaxies could be driven either by accretion of small gas-rich satellites or through *largely* dry equal mass mergers. Simulations of binary mergers at low redshift (Peirani, Kaviraj et al., in prep) indicate that galaxies on the broad *UV* red sequence can be reproduced by ‘minor’ mergers that have mass ratios between 1:6 and 1:10 and where the accreted satellites have high gas fractions ( $> 20$  percent). While it is difficult to discriminate between gas-rich satellite accretion and largely dry major mergers based on the RSF values alone (since both scenarios can supply equal amounts of gas), the favoured mechanism for RSF in the red sequence could possibly be deduced by studying the rates of minor and *red* major mergers at the redshifts sampled by this study. In a recent work, Bell et al. (2006) found that 12 out of 379 galaxies ( $\sim 3$  percent) in the E-CDFS *optical* red sequence are involved in major mergers (mass ratios greater than 1:4) and deduced that luminous ( $M(V) < -20.5$ ) early-types may have undergone 0.5-2 major dry mergers since  $z \sim 0.7$ . It therefore seems unlikely that major mergers alone can account for virtually the entire *UV* red sequence hosting low level RSF. Minor mergers (which are predicted to be more frequent in the hierarchical model) should therefore play a significant part in broadening the red sequence.

Early-types residing in the blue cloud necessarily require a more gas-rich formation scenario and a likely mechanism for creating these objects are gas-rich equal mass mergers. It is worth noting here that galaxies in the ‘possible early-type’ category almost exclusively inhabit the blue cloud (see Figure 3) and some appear to show asymmetries in their structure that may be indicative of a recent interaction (see the examples in Figure 2). It is reasonable to speculate that, given their largely spheroidal appearance and blue colours, some of the ‘possible early-types’ may be precursors of the relaxed early-type population in the blue cloud, implying that these blue early-types may also have had gas-rich interactions in the recent past. It is possible that the morphological signatures of the interactions are not visible in the images but the high stellar mass fraction formed in the burst imparts the (spheroidal) remnant with its observed blue *UV* colour. Finally, it is worth noting that if the vigorous star formation episode in these galaxies is quenched by e.g. SN or AGN feedback (Kaviraj et al. 2007), the galaxies will naturally evolve onto the red sequence. Therefore a small fraction of the broad red sequence could consist of such galaxies in the process of migration. However, since the migration is towards both redder colours and fainter magnitudes, this would affect a negligible part of the red sequence in this study due to the lack of red galaxies which have  $m(R) > 24$  in this sample (see bottom panel of Figure 3).

In summary, it seems reasonable to speculate that the broadness of the red sequence is driven by a combination

of condensation from the hot gas reservoirs coupled with accretion of gas-rich satellites (and to a lesser extent dry equal mass mergers), while early-types on the blue cloud are formed through gas-rich equal mass mergers that impart the remnant with its spheroidal morphology and leads to the high observed values of RSF.

The RSF values derived in this study have some interesting implications for the alpha-enhancement ( $[\alpha/Fe]$ ) observed in the spectra of nearby early-type galaxies. Massive early-types at low redshift frequently exhibit super-solar values of alpha-enhancement ( $[\alpha/Fe] \sim 0.3$  dex), which indicates that the bulk of the star formation in these galaxies takes place over a timescale shorter than the typical onset time of Type Ia supernovae (SN). While alpha elements (such as  $Mg$ ) are provided by Type II SN that appear on very short timescales of  $\sim 10^6$  yrs, the bulk of the  $Fe$  is supplied by Type Ia ejecta which are expected to appear after typical timelags of  $\sim 1$  Gyr. Hence, if star formation takes place over timescales greater than a Gyr, subsequent generations of stars incorporate the  $Fe$  injected into the inter-stellar medium, resulting in a decrease in the alpha-enhancement and  $[\alpha/Fe]$  values that reflect those in the solar neighbourhood.

It is instructive to estimate how much dilution we would expect in the early-type population from the RSF values derived in this study. If we assume that (a) the bulk stellar mass forming at high redshift is indeed created over a short timescale and has an alpha-enhancement characteristic of monolithic collapse ( $[\alpha/Fe] \sim 0.3$  dex) and (b) the rest of the mass forms over a longer timescale, at lower redshifts ( $z < 1$ ) and has an alpha-enhancement characteristic of the solar neighbourhood, then the mass-weighted  $[\alpha/Fe]$  at  $z \sim 0$  can be expressed approximately as

$$[\alpha/Fe] \sim (1 - f) \cdot [\alpha/Fe]_{ML} + f \cdot [\alpha/Fe]_{\odot}, \quad (1)$$

where  $f$  is the total mass fraction of stars formed at low redshifts ( $z < 1$ ),  $[\alpha/Fe]_{ML}$  is the alpha-enhancement of a ‘monolithic collapse’ type starburst and  $[\alpha/Fe]_{\odot}$  is the alpha-enhancement characteristic of the solar neighbourhood.

A strict monolithic collapse would create a stellar population with  $[\alpha/Fe] \sim 0.3$  dex (see e.g. top right panel of Kaviraj et al. 2006c). Since the observed  $[\alpha/Fe]$  values in early-type systems typically tend to be in excess of 0.2 (e.g. Thomas et al. 1999), Eqn (1) indicates that, with the stellar mass fractions expected to form in the bulk of the early-type population after  $z \sim 1$  (< 13 percent), the inferred alpha-enhancements in these galaxies should not deviate significantly from the monolithic value. While Eqn (1) is approximate, the RSF values we have derived in this study are in agreement with the observed alpha-enhancements of the local early-type galaxy population.

The sensitivity of the rest-frame  $UV$  spectrum to the recent SFH allows us sample the build-up of the SFH curve of galaxy populations over time. Clearly, access to the rest-frame  $UV$  over a large redshift range allows us to reconstruct the SFH curve with a reasonable degree of accuracy. While this study, together with similar work at low redshift (Kaviraj et al. 2006b), are the first attempts at such a reconstruction, future studies using the rest-frame  $UV$  are keenly anticipated, especially at higher redshifts ( $z > 2$ ) where massive early-type galaxies are in the process of or

have just completed their major episodes of star formation and assembly.

## ACKNOWLEDGEMENTS

We are grateful to Roger Davies and Rachel Somerville for numerous discussions which improved the quality of this work. Seong-Hee Kim is thanked for generously providing sample metallicity distribution functions from his galaxy formation models. Rob Kennicutt, Caina Hao, Chris Wolf, Claudia Maraston and Daniel Thomas are thanked for useful comments. SK acknowledges a Leverhulme Early-Career Fellowship, a BIPAC fellowship and a Junior Research Fellowship from Worcester College, University of Oxford.

## REFERENCES

- Adelman-McCarthy J. K., SDSS collaboration 2006, *ApJS*, 162, 38
- Andreon S., Lobo C., Iovino A., 2004, *MNRAS*, 349, 889
- Arnouts S., Vandame B., Benoist C., Groenewegen M. A. T., da Costa L., Schirmer M., Mignani R. P., Slijkhuis R., Hatziminaoglou E., Hook R., Madejsky R., Rit e C., Wicenec A., 2001, *A&A*, 379, 740
- Barnes J. E., Hernquist L., 1992a, *ARAA*, 30, 705
- Barnes J. E., Hernquist L., 1992b, *Nature*, 360, 715
- Barnes J. E., Hernquist L., 1996, *ApJ*, 471, 115
- Bell E. F., Naab T., McIntosh D. H., Somerville R. S., Caldwell J. A. R., Barden M., Wolf C., Rix H.-W., Beckwith S. V., Borch A., H aussler B., Heymans C., Jahnke K., Jooe S., Koposov S., Meisenheimer K., Peng C. Y., Sanchez S. F., Wisotzki L., 2006, *ApJ*, 640, 241
- Bell E. F., Wolf C., Meisenheimer K., Rix H.-W., Borch A., Dye S., Kleinheinrich M., Wisotzki L., McIntosh D. H., 2004, *ApJ*, 608, 752
- Bender R., 1997, in *ASP Conf. Ser. 116: The Nature of Elliptical Galaxies; 2nd Stromlo Symposium Structure; Formation and Ages of Elliptical Galaxies*. pp 11–+
- Bernardi M., the SDSS collaboration 2003, *AJ*, 125, 1817
- Binney J., 2004, *MNRAS*, 347, 1093
- Borch A., Meisenheimer K., Bell E. F., Rix H.-W., Wolf C., Dye S., Kleinheinrich M., Kovacs Z., Wisotzki L., 2006, *A&A*, 453, 869
- Bower R. G., Kodama T., Terlevich A., 1998, *MNRAS*, 299, 1193
- Bower R. G., Lucey J. R., Ellis R., 1992, *MNRAS*, 254, 589
- Bruzual G., Charlot S., 2003, *MNRAS*, 344, 1000
- Bundy K., Ellis R. S., Conselice C. J., Taylor J. E., Cooper M. C., Willmer C. N. A., Weiner B. J., Coil A. L., Noeske K. G., Eisenhardt P. R. M., 2006, *ApJ*, 651, 120
- Butcher H., Oemler A., 1984, *ApJ*, 285, 426
- Calzetti D., Armus L., Bohlin R. C., Kinney A. L., Koornneef J., Storchi-Bergmann T., 2000, *ApJ*, 533, 682
- Cardelli J. A., Clayton G. C., Mathis J. S., 1989, *ApJ*, 345, 245
- Chiosi C., Carraro G., 2002, *MNRAS*, 335, 335
- Cole S., Lacey C. G., Baugh C. M., Frenk C. S., 2000, *MNRAS*, 319, 168
- Couch W. J., Barger A. J., Smail I., Ellis R. S., Sharples R. M., 1998, *ApJ*, 497, 188

- Cowie L. L., Songaila A., Hu E. M., Cohen J. G., 1996, *AJ*, 112, 839
- de Zeeuw P. T., Bureau M., Emsellem E., Bacon R., Carollo C. M., Copin Y., Davies R. L., Kuntschner H., Miller B. W., Monnet G., Peletier R. F., Verolme E. K., 2002, *MNRAS*, 329, 513
- Dressler A., 1980, *ApJ*, 236, 351
- Dressler A., Oemler A. J., Couch W. J., Smail I., Ellis R. S., Barger A., Butcher H., Poggianti B. M., Sharples R. M., 1997, *ApJ*, 490, 577
- Eggen O. J., Lynden-Bell D., Sandage A. R., 1962, *ApJ*, 136, 748
- Ellis R. S., Abraham R. G., Dickinson M., 2001, *ApJ*, 551, 111
- Ellis R. S., Smail I., Dressler A., Couch W. J., Oemler A. J., Butcher H., Sharples R. M., 1997, *ApJ*, 483, 582
- Forbes D. A., Ponman T. J., Brown R. J. N., 1998, *ApJ*, 508, L43
- Franx M., 1993, *PASP*, 105, 1058
- Franx M., 1995, in van der Kruit P. C., Gilmore G., eds, *IAU Symp. 164: Stellar Populations Measuring the Evolution of the M/L Ratio from the Fundamental Plane*. pp 269–+
- Fukugita M., Nakamura O., Turner E. L., Helmboldt J., Nichol R. C., 2004, *ApJL*, 601, L127
- Gawiser E., MUSYC collaboration 2006, *ApJS*, 162, 1
- Giavalisco M., GOODS collaboration 2004, *ApJ*, 600, L93
- Gladders M. D., Lopez-Cruz O., Yee H. K. C., Kodama T., 1998, *ApJ*, 501, 571
- Hatton S., Devriendt J. E. G., Ninin S., Bouchet F. R., Guiderdoni B., Vibert D., 2003, *MNRAS*, 343, 75
- Hernquist L., 1993, in Shull J. M., Thronson H. A., eds, *ASSL Vol. 188: The Environment and Evolution of Galaxies* pp 327–+
- Israel F. P., 1998, *A&AR*, 8, 237
- Jorgensen I., Franx M., Kjaergaard P., 1996, *MNRAS*, 280, 167
- Kaviraj S., Devriendt J. E. G., Ferreras I., Yi S. K., 2005, *MNRAS*, 360, 60
- Kaviraj S., Devriendt J. E. G., Ferreras I., Yi S. K., Silk J., 2006a, *MNRAS*; astro-ph/0602347
- Kaviraj S., GALEX Science Team 2006b, *ApJ* (accepted - to appear in GALEX dedicated issue in Dec 2007)
- Kaviraj S., Kirkby L. A., Silk J., Sarzi M., 2007, astro-ph/0707.3570
- Kaviraj S., Rey S.-C., Rich R. M., Lee Y., Yoon S.-J., Yi S. K., 2006c, *MNRAS* in press; astro-ph/0601050
- Khochfar S., Burkert A., 2001, *ApJ*, 561, 517
- Khochfar S., Burkert A., 2003, *ApJ*, 597, L117
- Khochfar S., Burkert A., 2005, *MNRAS*, 359, 1379
- Khochfar S., Silk J., 2006, *MNRAS*, 370, 902
- Larson R. B., 1974, *MNRAS*, 166, 385
- Le Fèvre O., VVDS collaboration 2004, *A&A*, 417, 839
- Malin D. F., Carter D., 1983, *ApJ*, 274, 534
- Margoniner V. E., de Carvalho R. R., Gal R. R., Djorgovski S. G., 2001, *ApJL*, 548, L143
- Martin D. C., GALEX collaboration 2005, *ApJ*, 619, L1
- Menanteau F., Abraham R. G., Ellis R. S., 2001, *MNRAS*, 322, 1
- Peebles P. J. E., 2002, in *ASP Conf. Ser. 283: A New Era in Cosmology* pp 351–+
- Rix H.-W., GEMS collaboration 2004, *ApJS*, 152, 163
- Sadler E. M., Gerhard O. E., 1985, 214, 177
- Saglia R. P., Colless M., Baggle G., Bertschinger E., Burstein D., Davies R. L., McMahan R. K., Wegner G., 1997, in Arnaboldi M., Da Costa G. S., Saha P., eds, *ASP Conf. Ser. 116: The Nature of Elliptical Galaxies; 2nd Stromlo Symposium The EFAR Fundamental Plane*. pp 180–+
- Sarzi M., Falcón-Barroso J., Davies R. L., Bacon R., Bureau M., Cappellari M., de Zeeuw P. T., Emsellem E., Fathi K., Krajnović D., Kuntschner H., McDermid R. M., Peletier R. F., 2006, *MNRAS*, 366, 1151
- Schawinski K., Khochfar S., Kaviraj S., Yi S. K., GALEX collaboration 2006, *Nature*, 442, 888
- Schweizer F., Seitzer P., 1992, *AJ*, 104, 1039
- Schweizer F., Seitzer P., Faber S. M., Burstein D., Dalle Ore C. M., Gonzalez J. J., 1990, *ApJ*, 364, L33
- Serra P., Trager S. C., van der Hulst J. M., Oosterloo T. A., Morganti R., 2006
- Spergel D. N., WMAP collaboration 2007, *ApJS*, 170, 377
- Stanford S. A., Eisenhardt P. R. M., Dickinson M., 1998, *ApJ*, 492, 461
- Thomas D., Greggio L., Bender R., 1999, *MNRAS*, 302, 537
- Tomita A., Aoki K., Watanabe M., Takata T., Ichikawa S.-i., 2000, *AJ*, 120, 123
- Toomre A., 1977, in Tinsley B. M., Larson R. B., eds, *Evolution of Galaxies and Stellar Populations* pp 401–+
- Trager S. C., Faber S. M., Worthey G., González J. J., 2000a, *AJ*, 119, 1645
- Trager S. C., Faber S. M., Worthey G., González J. J., 2000b, *AJ*, 120, 165
- Tran H. D., Tsvetanov Z., Ford H. C., Davies J., Jaffe W., van den Bosch F. C., Rest A., 2001, *AJ*, 121, 2928
- van der Wel A., Franx M., Illingworth G. D., van Dokkum P. G., 2007, astro-ph/0705.3394; accepted for publication in *ApJ*, 705
- van Dokkum P. G., 2005, *AJ*, 130, 2647
- van Dokkum P. G., Franx M., 1996, *MNRAS*, 281, 985
- van Dokkum P. G., Franx M., 2001, *ApJ*, 553, 90
- van Dokkum P. G., Franx M., Fabricant D., Illingworth G. D., Kelson D. D., 2000, *ApJ*, 541, 95
- van Dokkum P. G., Franx M., Fabricant D., Kelson D. D., Illingworth 1999, *ApJ*, 520, L95
- Virani S. N., Treister E., Urry C. M., Gawiser E., 2006, *AJ*, 131, 2373
- Wolf C., Bell E. F., McIntosh D. H., Rix H.-W., Barden M., Beckwith S. V. W., Borch A., Caldwell J. A. R., Häussler B., Heymans C., Jahnke K., Jogee S., Meisenheimer K., Peng C. Y., Sánchez S. F., Somerville R. S., Wisotzki L., 2005, *ApJ*, 630, 771
- Wolf C., Meisenheimer K., Kleinheinrich M., Borch A., Dye S., Gray M., Wisotzki L., Bell E. F., Rix H.-W., Cimatti A., Hasinger G., Szokoly G., 2004, *A&A*, 421, 913
- Worthey G., 1994, *ApJS*, 95, 107
- Yi S., Demarque P., Oemler A. J., 1997, *ApJ*, 486, 201
- Yi S., Lee Y.-W., Woo J.-H., Park J.-H., Demarque P., Oemler A. J., 1999, *ApJ*, 513, 128
- Yi S. K., 2003, *ApJ*, 582, 202